MCB
Journals.ASM.org

Human DEAD Box Helicase 3 Couples IκB Kinase ε to Interferon Regulatory Factor 3 Activation

Lili Gu, Anthony Fullam, Ruth Brennan, Martina Schröder

Institute of Immunology, National University of Ireland Maynooth, Maynooth, County Kildare, Ireland

The human DEAD box protein 3 (DDX3) has been implicated in different processes contributing to gene expression. Interestingly, DDX3 is required as an essential host factor for the replication of HIV and hepatitis C virus (HCV) and is therefore considered a potential drug target. On the other hand, DDX3 interacts with IκB kinase ε (IKKε) and TANK-binding kinase 1 (TBK1) and contributes to the induction of antiviral type I interferons (IFNs). However, the molecular mechanism by which DDX3 contributes to IFN induction remains unclear. Here we show that DDX3 mediates phosphorylation of interferon regulatory factor 3 (IRF3) by the kinase IKKε. DDX3 directly interacts with IKKε and enhances its autophosphorylation and activation. IKKε then phosphorylates several serine residues in the N terminus of DDX3. Phosphorylation of DDX3 at serine 102 (S102) is required for recruitment of IRF3 to DDX3, facilitating its phosphorylation by IKKε. Mutation of S102 to alanine disrupted the interaction between DDX3 and IRF3 but not that between DDX3 and IKKε. The S102A mutation failed to enhance *ifnb* promoter activation, suggesting that the DDX3-IRF3 interaction is crucial for this effect. Our data implicates DDX3 as a scaffolding adaptor that directly facilitates phosphorylation of IRF3 by IKKε. DDX3 might thus be involved in pathway-specific activation of IRF3.

The human DEAD box RNA helicase DDX3 is a multifunctional cellular protein which has been implicated in various processes linked to gene expression (1). Its RNA helicase activity is coopted by viruses that require DDX3 as an essential host factor for their replication, such as HIV and HCV (2–4). In contrast, we and others have previously demonstrated that DDX3 contributes to antiviral innate immune signaling pathways leading to *ifnb* induction (5–9). This function of DDX3 is independent of its ATPase and helicase activity (6, 7). *ifnb* promoter induction requires activation of the transcription factors IRF3 and IRF7, which occurs only downstream of certain, mostly antiviral, pattern recognition receptors (PRRs). Antiviral PRRs comprise the endosomal Toll-like receptors TLR3, TLR7, TLR8, and TLR9, cytosolic RIG-like helicases (RLHs), and several newly discovered cytosolic DNA receptors (10). These receptors recognize different species of viral nucleic acids and induce type I IFNs in response (11). TLR3 and TLR4 engage the TRIF (TIR domain-containing adaptor inducing IFN-β)-dependent pathway for activation of IRF3 (12). In this pathway, phosphorylation-dependent activation of IRF3 is mediated by the IKK-related kinases TBK1 and IKKε (13, 14). The RLHs also utilize TBK1 and IKKε for IRF3 activation after engaging the adaptor molecule MAVS (mitochondrial antiviral signaling) (15, 16). DNA receptors activate IRF3 through TBK1 and the adaptor molecule STING (stimulator of IFN genes).

While these signaling pathways converge on IKKε and TBK1 for IRF3 activation, not all receptors that activate IKKε and/or TBK1 lead to IRF3 activation (17). This suggests that additional factors are required for linking the activated kinases to their substrate IRF3.

We previously showed that DDX3 interacts with IKKε following activation of the RIG-I (retinoic acid-inducible) pathway and that it contributes to *ifnb* promoter induction downstream of PRRs that utilize IKKε and TBK1 for IRF3 activation (6). Soulat et al. published similar results regarding a role for DDX3 in *ifnb* induction and demonstrated that DDX3 interacts with and is phosphorylated by TBK1 (7). They also showed binding of DDX3 to the *ifnb* promoter and hypothesized that phosphorylated DDX3 directly mediates *ifnb* transcription (7). Interestingly, the function of DDX3 in *ifnb* induction is targeted by viral immune evasion strategies that inhibit the induction of this potent antiviral cytokine. For example, we previously showed that the vaccinia virus (VACV) protein K7 antagonizes DDX3 by binding to its N-terminal tail region, which is required for *ifnb* promoter induction (6, 18, 19). The hepatitis B virus (HBV) polymerase (Pol) is another viral protein that interacts with DDX3. Initially it was shown that DDX3 gets incorporated into the viral nucleocapsid and blocks viral replication (20). More recently, it was demonstrated that HBV Pol targets DDX3 in much the same way as K7: it blocks its interaction with IKKε/TBK1 and consequently inhibits IRF3 activation and *ifnb* induction (8, 9). Another recent study also confirmed a role for DDX3 in *ifnb* induction but placed DDX3 further upstream in the signaling pathway. Oshiumi et al. suggested that DDX3 directly senses HCV RNA and then triggers MAVS-dependent signaling (5). In a follow-up study, those authors also suggested that the HCV core protein, which had previously been shown to interact with DDX3 (21–23), blocks the interaction between DDX3 and MAVS and thereby prevents initiation of this pathway (24). In summary, there is now strong evidence that human DDX3 contributes to *ifnb* promoter induction, in particular with respect to the RIG-I pathway. However, its exact placement in the signaling pathway and its mechanism of action are still unclear. Several studies, including ours, placed DDX3 downstream of TBK1/IKKε (6–9). However, Oshiumi et al. placed it upstream of MAVS, as a viral RNA sensor that functions in conjunction with RIG-I/MAVS (5, 24). It is also unclear whether the

Received 27 November 2012 **Returned for modification** 15 January 2013
Accepted 1 March 2013
Published ahead of print 11 March 2013
Address correspondence to Martina Schröder, martina.schroeder@nuim.ie.

doi:10.1128/MCB.01603-12

effect of DDX3 is located upstream of IRF3 activation and/or whether it binds directly to the *ifnb* promoter to enhance transcription (6, 7). The present study therefore aimed at placing DDX3 more firmly in the signaling pathway(s) leading to *ifnb* induction by dissecting its molecular interaction with IKKε and the functional consequences of this interaction. We show here that DDX3 mediates IKKε activation and then couples the active kinase to its substrate, the transcription factor IRF3. Mechanistically, DDX3 therefore acts as a downstream scaffolding adaptor that links IKKε and IRF3.

MATERIALS AND METHODS

Plasmids, recombinant proteins, and antibodies. The expression constructs pCMV-HA-DDX3, pCMV-Myc-DDX3, pHis-DDX3, HA-K7, and His-K7 were described in our previous study (6). pCMV-HA-DDX3 and pHis-Parallel2-DDX3 point mutations were introduced by following the instructions for the QuikChange site-directed mutagenesis kit (Agilent), except that Pfusion HiFi polymerase was used (New England BioLabs). TBK1-Flag, IKKε-Flag, IKKε KD-Flag (kinase dead, K48A), and IRF3-Flag were kind gifts from Kate Fitzgerald (University of Massachusetts Medical School, Worcester, MA). IKKε-Flag truncation constructs were generated by amplifying the relevant sequences by PCR from IKKε-Flag and inserting them into pFlag-CMV2 (Sigma-Aldrich).

DDX3(1–408) (a DDX3 construct consisting of amino acids [aa] 1 to 408), DDX3(409–662), DDX3(139–408), and DDX3(1–139) were described previously (6). DDX3(80–408), DDX3(100–408), DDX3(110–408), DDX3(120–408), and DDX3(130–408) were constructed by amplifying the relevant sequences by PCR from pCMV-HA-DDX3 and inserting them into pHisparallel2 or pCMV-HA vectors. Full-length DDX3 was subcloned from pHis-DDX3 into pGSTParallel2 using the EcoRI and SalI restriction sites to generate the bacterial expression construct pGST-DDX3. pHis-Rab14 and DDX3(5–172) constructs were kind gifts from Amir Khan (Trinity College Dublin). Glutathione S-transferase (GST)–IRF3 (aa 380 to 427) peptides and constructs were kindly provided by John Hiscott and Qiang Sun (McGill University, Montreal, Canada). A construct for full-length His-IRF3 was provided by Marion Butler (NUI Maynooth). Purified recombinant protein kinase GST-IKKε was purchased from Proqinase (Freiburg, Germany). The antibodies used were anti-Flag M2 monoclonal antibody (MAb) (Sigma-Aldrich), anti-Myc MAb clone 9E10 (Sigma-Aldrich), antihemagglutinin (anti-HA) MAb (Covance), anti-DDX3 (Santa Cruz or Bethyl Laboratories), anti-IKKε (Abcam, Cambridge, United Kingdom), anti-IRF3 (IBL), anti-phospho-Ser396-IRF3 (Cell Signaling Technology), anti-phospho-Ser172-TBK1/IKKε and anti-phospho-Ser172 IKKε (Cell Signaling Technology), anti-His (Sigma-Aldrich), and anti-GST (Promega).

Cell culture and transfection. HEK293T and A549 cells were maintained in Dulbecco's modified Eagle medium (DMEM) with Glutamax (Gibco), supplemented with 10% fetal calf serum and 50 ng/ml gentamicin (Sigma-Aldrich). Transient DNA transfections for immunoprecipitations and pulldowns were performed using the calcium phosphate method. The total amount of DNA was kept constant by addition of empty vector.

siRNA knockdown of DDX3. For small interfering RNA (siRNA) knockdown of endogenous human DDX3, two different stealth RNA interference (RNAi) oligonucleotides, DDX3-1 (GGGAGAAAUUAUCAUGGGAAACAUU) (HSS102712; Invitrogen) and DDX3-2 (UUCAACAAGAAGAUCCAACAAAUCC) (HSS102713; Invitrogen), with a control oligonucleotide of matched GC content (all supplied by Invitrogen), were used. Approximately 60,000 HEK293T cells were transfected with RNAi (50 pmol) in individual wells of a 24-well plate using Lipofectamine 2000 (Invitrogen), according to the manufacturer's instructions. At 48 h after transfection, cell lysates were prepared and analyzed by SDS-PAGE and immunoblotting.

GST or His pulldown assays. Bacterial expression constructs for His- or GST-tagged proteins were transformed into *Escherichia coli* BL21(DE3). Protein expression was induced by IPTG (isopropyl-β-D-thiogalactopyranoside), and recombinant proteins were purified using either nickel-agarose or glutathione-Sepharose (both from Chromatrin Ltd., Dublin, Ireland). For pulldowns, equal amounts of the different His- or GST-tagged fusion proteins were used, as estimated by SDS-PAGE and Coomassie staining prior to use. Cell lysates containing Flag-tagged protein expressed in HEK293T cells, 0.1 μg of GST-IKKε, or 0.5 μg of purified recombinant protein were incubated with relevant purified His- or GST-tagged proteins immobilized on nickel-agarose or glutathione-Sepharose, respectively. Protein complexes were precipitated and washed thoroughly before being subjected to SDS-PAGE and Western blot analysis.

Coimmunoprecipitation assays. Coimmunoprecipitations were performed from cell lysates of transiently transfected HEK293T or A549 cells, which were harvested 24 h after transfection. Cells were lysed in immunoprecipitation (IP) lysis buffer (50 mM HEPES [pH 7.4], 150 mM NaCl, 2 mM EDTA, 1% NP-40, 10% glycerol, 10 mM NaF, 1 mM sodium orthovanadate, protease inhibitors). Cell lysates were incubated with 20 μl of Flag-M2 agarose (Sigma-Aldrich) or protein A/G agarose (Santa Cruz) that had been precoupled with relevant antibodies at 4°C overnight and blocked with 5% bovine serum albumin (BSA). The immunoprecipitated protein complexes were washed thoroughly and then eluted by boiling in Laemmli sample buffer before being subjected to SDS-PAGE and Western blot analysis.

***In vitro* kinase assays.** *In vitro* kinase assays were carried out either with Flag-tagged IKKε or TBK1 immunoprecipitated from lysates of transfected HEK293T cells or with 55 ng of purified recombinant GST-IKKε (Proqinase). These were incubated with recombinant substrates in kinase assay buffer (50 mM HEPES [pH 7.5], 5 mM glycerophosphate, 2 mM dithiothreitol, 0.1 mM Na_3VO_4, 10 mM $MgCl_2$) in the presence of 20 μM unlabeled ATP for 30 min at 30°C. Samples were analyzed by SDS-PAGE and Western blot analysis with relevant antibodies. Alternatively, kinase assays were carried out in the presence of 10 μM unlabeled ATP and 5 μCi of [γ-^{32}P]ATP. Samples were then analyzed by SDS-PAGE and autoradiography.

Determination of phosphorylation sites by mass spectrometry. 0.5 μg of His-DDX3 (full-length) or His-DDX3 (1 to 408) were phosphorylated *in vitro* using recombinant protein kinase GST-IKKε as described above. Samples were then subjected to SDS-PAGE and Coomassie staining. Bands that corresponded to His-DDX3 (full length)- and His-DDX3(1–408)-specific bands were cut out and reductively alkylated in-gel with 10 mM dithiothreitol (DTT) and 50 mM iodoacetamide. Gel bands were then digested with trypsin solution (20 μl of 12.5 μg/ml trypsin [Roche] in 20 mM ammonium bicarbonate) overnight. The digested peptides were extracted, dried in a speed vac, and suspended in 50 μl of 1% formic acid. A 15-μl portion of the peptide extract was injected onto a Dionex U3000 nanoLC system with a 75-μm by 15-cm C_{18} PepMap column using a 65-min linear gradient from 5 to 35% B (90% acetonitrile in 0.1% formic acid). The instrument method used was a TOP 15 method (MS survey scan followed by 15 ion trap tandem mass spectrometry [IT-MSMS] scans) with multistage activation (MSA). Data were extracted with Proteome Discoverer (v. 1.3), and database searching was done using the Mascot search engine (v. 2.3.2).

Reporter gene assays. *ifnb* promoter induction was measured in HEK293T cells seeded into 96-well plates (2×10^4 cells per well) and transfected 24 h later with expression vectors and luciferase reporter gene constructs, using GeneJuice (Merck/Millipore). Sixty nanograms of an *ifnb* promoter firefly luciferase reporter gene construct was used in conjunction with 20 ng of a pGL3-*Renilla* luciferase construct (both provided by Andrew Bowie, Trinity College Dublin). The total amount of DNA transfected was kept constant at 230 ng/well by addition of matching empty vector DNA. Firefly and *Renilla* luciferase activity was measured 24 h after transfection. *Renilla* luciferase readings were used to normalize for transfection efficiency. Data are expressed as mean fold induction ± standard deviations (SD) relative to control levels for an individual experi-

ment performed in triplicate. Remaining cell lysates from each triplicate were pooled and subjected to SDS-PAGE and Western blot analysis to show expression levels of transfected DDX3 and IKKε.

Data representation and statistical analysis. All data shown are representative of at least two independent repeat experiments, and most are representative of 3 to 5 repeat experiments. Luciferase reporter gene assays are representative of at least 3 independent repeat experiments.

Statistical analysis was carried out using a two-tailed unpaired Student's *t* test and SPSS software.

RESULTS

DDX3 enhances activation of IKKε and IRF3. First, we wanted to confirm whether DDX3 affects activation of IRF3 or whether it exerts its effect downstream of or in parallel with IRF3. We had previously shown that DDX3 knockdown affects an IRF3 transactivation assay based on a GAL4-IRF3 fusion protein used in conjunction with a GAL4-dependent reporter construct (6). VACV K7 and HBV Pol, both of which target DDX3, have been shown to inhibit IRF3 activation, which provides indirect evidence for involvement of DDX3 in IRF3 activation (6, 8, 9). However, it has also been suggested that DDX3 binds directly to the *ifnb* promoter and has no interaction with IRF3 (7). In order to test for an effect of DDX3 on IKKε and IRF3 activation, we used small interfering RNA (siRNA) to knock down endogenous human DDX3. Flag-IKKε was then expressed in these cells, followed by immunoprecipitation and *in vitro* kinase assays with recombinant glutathione-*S*-transferase (GST)-IRF3 (aa 380 to 427). DDX3 knockdown with two different siRNA oligonucleotides led to a clear reduction of IKKε-induced phosphorylation of IRF3 at serine 396 (Fig. 1A). S396 is one of the key phosphorylation sites for IKKε/TBK1 and is required for IRF3 activation (25). This finding suggested that IKKε activation or activity is decreased in the absence of DDX3. Consistent with this, the addition of recombinant DDX3 enhanced IKKε-mediated S396 phosphorylation of IRF3 in kinase assays with recombinant IKKε (Fig. 1B). We also noticed that the presence of DDX3 induced a higher-molecular-weight form of IKKε (Fig. 1B, asterisk), which likely represents a phosphorylated form of IKKε. We therefore tested whether DDX3 enhances phosphorylation of IKKε at serine 172. S172 is located in the activation loop of IKKε and required for its activation (26). Indeed, S172 phosphorylation of IKKε was enhanced in the presence of DDX3 (Fig. 1C, top, lanes 2 and 4). DDX3 also enhanced IKKε-mediated IRF3 phosphorylation in the same experiment (Fig. 1C, third panel, lane 4), likely as a consequence of increased IKKε activity. When DDX3 was coexpressed in HEK293 cells with small amounts of exogenous IKKε, DDX3 also enhanced IKKε and IRF3 phosphorylation (Fig. 1D). Furthermore, exogenous expression of DDX3 enhanced Sendai virus (SeV)-induced phosphorylation of IRF3 (Fig. 1E). Finally, we wanted to confirm that endogenous DDX3 is required for activation of endogenous IKKε and IRF3 following SeV stimulation. HEK293 cells have low levels of endogenous IKKε, and we therefore knocked down DDX3 expression in the human lung epithelial cell line A549. In A549 cells with DDX3 knockdown, S396 phosphorylation of IRF3 was reduced compared to that in cells treated with a control siRNA oligonucleotide (NC) (Fig. 1F, fifth panel). In experiments with recombinant or overexpressed IKKε (Fig. 1A to E), we used an antibody that recognizes pS172 in both TBK1 and IKKε. With the same antibody, we observed a clear reduction of endogenous pS172 TBK1/IKKε phosphorylation in cells treated with DDX3 siRNA (Fig. 1F, second panel). In addition, we used a newer antibody that is more specific for phosphorylated IKKε and saw a similar reduction in pS172 IKKε levels in DDX3 knockdown cells (Fig. 1F, third panel). As DDX3 also interacts with TBK1 (7), it is possible that DDX3 affects both TBK1 and IKKε activation. Our study focused on IKKε activation (because in our hands it is the stronger binding partner for DDX3), and we carried out a combination of experiments with recombinant, overexpressed, and endogenous IKKε. Our results clearly demonstrate that DDX3 acts at the level of IKKε and IRF3 by enhancing autophosphorylation of IKKε and (consequently) IRF3 phosphorylation.

DDX3 directly interacts with the scaffolding/dimerization domain of IKKε. The *in vitro* kinase assays whose results are shown in Fig. 1B and C were carried out with recombinant IKKε and DDX3, suggesting that DDX3 directly interacts with IKKε. We next carried out pulldown assays to confirm this and to map their interaction. The recombinant His-tagged DDX3 proteins we used for this analysis were the full-length protein (aa 1 to 662), the N-terminal domain (aa 1 to 408), the C-terminal domain (aa 409 to 662), and the N-terminal domain with a truncated N-terminal tail (aa 139 to 408). The 1–408 and 409–662 constructs split DDX3 at the linker region between its two RecA-like globular domains (27). We have previously shown that the flexible N-terminal tail region (aa 1 to 139) is required for the effect of DDX3 on the *ifnb* promoter (6), which is why we included the 139–408 truncation mutant.

Full-length recombinant His-DDX3, as well as its N-terminal (aa 1 to 408) and C-terminal (aa 409 to 662) domains, pulled down GST-tagged recombinant IKKε, confirming the direct interaction and suggesting that DDX3 contains at least two distinct interaction sites for IKKε (Fig. 2A). Interestingly, the 139–408 truncation of DDX3 did not interact with IKKε (Fig. 2A), indicating that the IKKε interaction is at least partially mediated by residues in the flexible N-terminal region of DDX3 that is required for *ifnb* promoter induction.

In Fig. 1, we have demonstrated that DDX3 enhances IKKε autoactivation. Other adaptor proteins that contribute to IKKε and TBK1 activation in cells are NAP1 (NAK-associated protein 1), TANK (TRAF family member-associated NF-κB activator) and Sintbad (similar to NAP1 TBK1 adaptor) (28), which have recently been shown to bind to the C-terminal region of IKKε (aa 684 to 716) and the corresponding region in TBK1 (29, 30). We therefore asked whether DDX3 interacts with IKKε in a similar manner. We transfected HEK293T cells with constructs for Myc-tagged DDX3 and a range of different Flag-tagged IKKε truncation mutants, followed by immunoprecipitation with an anti-Flag antibody. DDX3 interacted strongly with a truncated IKKε construct lacking the kinase and ubiquitin-like domains (aa 383 to 716), as well as constructs lacking the adaptor-binding region (aa 1 to 684 and 1 to 647) (Fig. 2B). DDX3 weakly interacted with a truncated IKKε containing the kinase and ubiquitin-like domains only (aa 1 to 383). We also performed a semiendogenous co-IP by transfecting HEK293T cells with truncated IKKε constructs, followed by immunoprecipitation of endogenous DDX3. Again, DDX3 interacted with all truncated IKKε constructs but only weakly with the 1-383 construct (Fig. 2C). We did not observe consistent differences in binding between the other IKKε truncations, suggesting that DDX3 binds mainly to a region between aa 383 and 647 in IKKε, which corresponds to its scaffolding/dimerization domain (SDD). The adaptor binding region (aa 684 to 716) was not required for DDX3 binding.

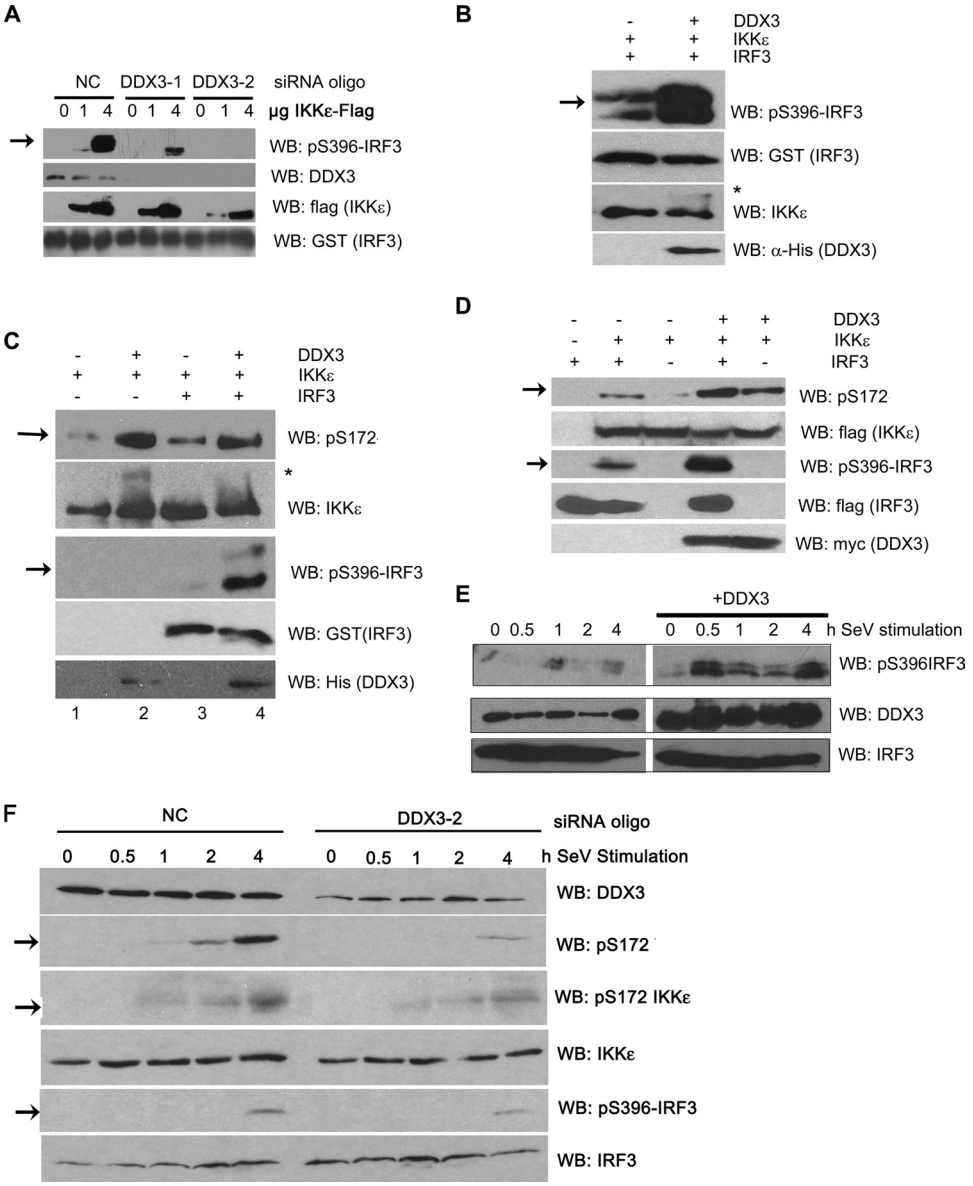

FIG 1 DDX3 enhances activation of IKKε and IRF3. (A) HEK293T cells were transfected with siRNAs against DDX3 (DDX3-1 and DDX3-2) or a negative-control oligonucleotide (NC). After 24 h, cells were transfected with a plasmid vector for Flag-IKKε or with an empty vector. Flag-IKKε was immunoprecipitated, and *in vitro* kinase assays were performed using recombinant GST-IRF3 (aa 380 to 427) as a substrate. IRF3 phosphorylation was detected with a phospho-specific antibody against serine 396 by Western blot (WB) analysis. (B and C) *In vitro* kinase assays were carried out with recombinant GST-IKKε and IRF3. Recombinant His-DDX3 was added where indicated. Phosphorylation of IKKε and IRF3 was detected with phospho-specific antibodies against S172 in IKKε and S396 in IRF3. The asterisk indicates a higher-molecular-weight band of IKKε. (D and E) HEK293T cells were transfected with expression constructs for myc-DDX3 and Flag-IRF3. (D) Cells were cotransfected with a Flag-IKKε construct or empty vector. (E) Cells were stimulated with SeV 24 h after transfection for the indicated length of time. (F) A549 cells were transfected with an siRNA oligonucleotide against DDX3 (DDX3-2) or a negative-control oligonucleotide (NC). After 48 h, cells were stimulated with SeV for the indicated length of time. Cell lysates were subjected to SDS-PAGE and WB analysis.

While the kinase and ubiquitin-like domains of IKKε are also not required for the interaction, DDX3 binds to this region weakly, presumably as a substrate for IKKε's kinase activity.

The N terminus of DDX3 is phosphorylated by IKKε. There is evidence that interaction with IKKε leads to phosphorylation of DDX3. Soulat et al. described DDX3 as a phosphorylation target of TBK1 (7), and we also observed the appearance of higher-molecular-weight forms of DDX3 after coexpression of DDX3 with IKKε but not with a kinase-inactive mutant of IKKε (6) (Fig. 3A). We carried out *in vitro* kinase assays with IKKε and recombinant DDX3 in order to confirm that DDX3 is a substrate of IKKε. Recombinant DDX3 was phosphorylated *in vitro* by recombinant IKKε (Fig. 3B). This phosphorylation was comparable in intensity to that of the bona fide IKKε substrate IRF3 in the same experiment (Fig. 3B). Because the N- and C-terminal domains of DDX3 both directly interacted with IKKε (Fig. 2A), we asked whether both domains are phosphorylated by IKKε. While we observed a very weak phosphorylation signal for the C-terminal domain of DDX3 (aa 409 to 662), the N-terminal domain (aa 1 to 408) was phosphorylated much more strongly (Fig. 3C). The N-terminal

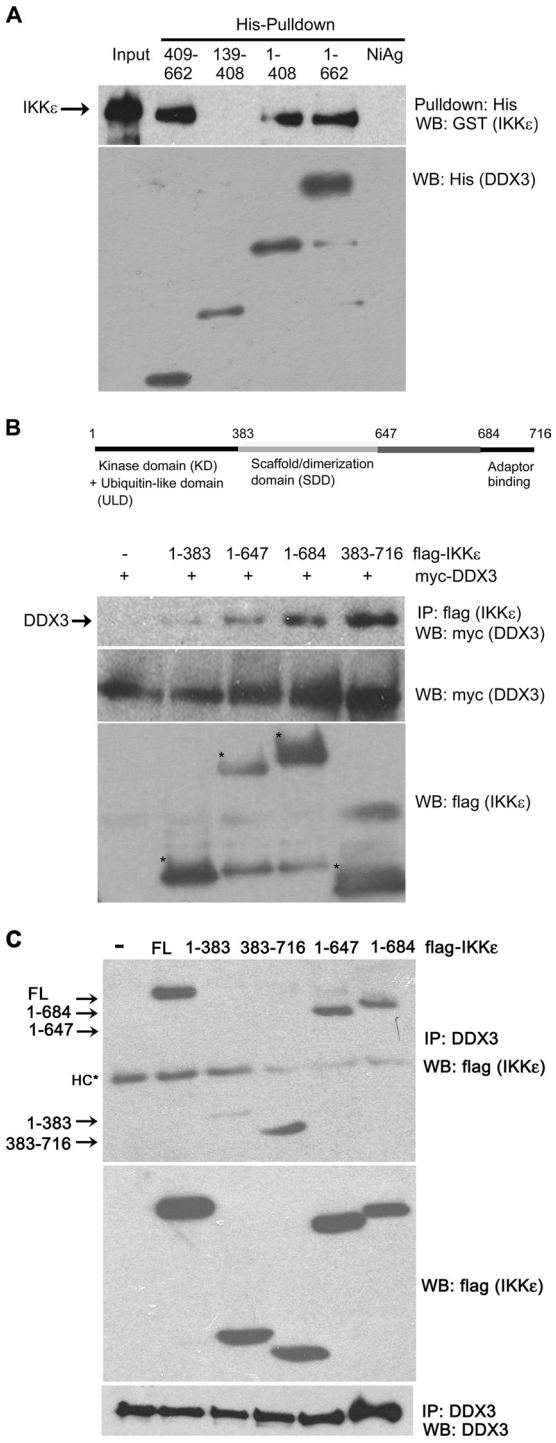

FIG 2 DDX3 directly interacts with the SDD domain of IKKε. (A) Purified recombinant full-length His-DDX3 or the indicated His-DDX3 truncation mutants were incubated with recombinant GST-IKKε. Following pulldown with nickel (Ni)-agarose, interacting proteins were subjected to SDS-PAGE and WB analysis. (B and C) HEK293T cells were transfected with constructs for Flag-IKKε or the indicated Flag-IKKε truncation mutants and Myc-DDX3 (panel B only). Cell lysates were subjected to immunoprecipitation (IP) with an anti-Flag (B) or anti-DDX3 (C) antibody, followed by SDS-PAGE and WB analysis. Asterisks mark bands of the correct molecular weight for the IKKε truncations (B). HC, antibody heavy chain band (C).

truncation mutant DDX3(139–408) failed to interact with IKKε (Fig. 2A), which suggested that the phosphorylation sites for IKKε might be contained in the N-terminal tail region. Therefore, we next used the isolated N-terminal region of DDX3 as a substrate. Polypeptides comprising aa 1 to 139 or aa 5 to 172 of DDX3 were strongly phosphorylated by IKKε in kinase assays, suggesting that this region indeed contains phosphorylation sites for IKKε (Fig. 3D and E). An unrelated His-tagged protein of a similar molecular weight (Rab14) served as a control and was not phosphorylated by IKKε (Fig. 3D). TBK1 appeared to phosphorylate the N-terminal domain of DDX3 to an extent similar to that exhibited by IKKε, as evidenced by the shift of DDX3(5–172) after nonradioactive kinase assays with immunoprecipitated IKKε or TBK1 (Fig. 3E).

Mapping of IKKε phosphorylation sites in DDX3. We next aimed at identifying the exact residues in DDX3 that are phosphorylation sites for IKKε. This was not a trivial task, considering that the N terminus of DDX3 (aa 1 to 172) contains 29 serine residues and the C-terminal SG-rich domain (aa 580 to 662) contains 20 serine residues, many of them arranged in clusters that are potential targets for IKKε phosphorylation.

Hutti et al. recently defined an IKKε consensus phosphorylation motif, which they generated using a positional scanning peptide library assay (31). Those authors kindly provided us with their Scansite matrix (31), which we used to scan the DDX3 protein sequence for IKKε consensus motifs (32). This revealed a large number of potential, if suboptimal, IKKε phosphorylation sites, mainly clustered in the N- and C-terminal serine-rich regions of DDX3. Due to our experimental evidence that the N-terminal tail region of DDX3 (aa 5 to 172) is strongly phosphorylated by IKKε, we focused on this region. Within this region, serine S71 had the best Scansite score (0.7571), followed by S82, S57, S70, S137, S58, S86, S23, S61, S152, S74, S28, S131, S62, S83, and S102 (1.1486). Of these, S82, S57, S86, S61, S152, S74, S28, S131, S62, S83, and S102 were also predicted to be phosphorylated by NetPhos 2.0 (score $>$ 0.75) (33). Due to this large number of potential phosphorylation sites, we carried out phosphorylation site mapping by mass spectrometry. For this analysis, we used full-length DDX3 and DDX3(1–408) that had been phosphorylated *in vitro* using recombinant IKKε. We separated the phosphorylated protein by SDS-PAGE and carried out a tryptic digest of the protein band, followed by analysis of the tryptic peptides by ion trap mass spectrometry (IT-MS). For full-length DDX3, the only significant hit we obtained was a phosphorylated peptide containing S70, S71, and S74. For DDX3(1–408), we obtained hits that matched phosphorylation sites at S152, at S70, S71, or S74, at S102 or S109, and at S82, S83, or S86 (Table 1). Based on these data and the Scansite predictions, we selected S71, S82, S83, S102, and S152 for serine-to-alanine substitution mutations. We generated single-alanine-substitution mutants for S71, S102, and S152, a double-alanine mutant for S82 and S83 (2A mutant), a triple-alanine mutant for S82, S83, and S102 (3A mutant), and a quadruple-alanine mutant for S71, S82, S83, and S102 (4A mutant). In kinase assays with IKKε, our single-alanine mutants displayed reductions in phosphorylation between ~32% for the S102A mutant and ~60% for the S71A and S152A mutants. For the 2A mutant, phosphorylation was reduced by ~50%, and the 3A and 4A mutants retained only ~35% of phosphorylation compared to the wild-type 1-408 truncation construct (Fig. 4A). These data suggest that the serine residues we identified are indeed phosphorylated by IKKε; however,

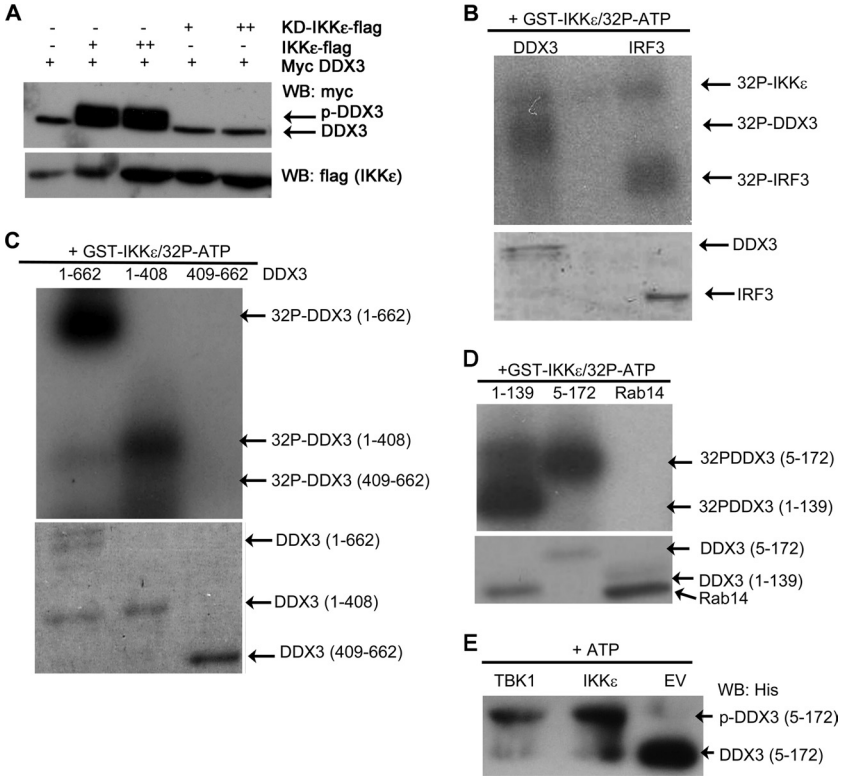

FIG 3 The N terminus of DDX3 is a direct phosphorylation target for IKKε. (A) HEK293T cells were transfected with constructs for Myc-DDX3 and 100 ng (+) or 250 ng (++) of a Flag-IKKε construct or 1,000 ng (+) or 1,800 ng (++) of a construct for a kinase-dead (KD) Flag-IKKε mutant (K38A). Cell lysates were subjected to SDS-PAGE and WB analysis. (B to D) For *in vitro* kinase assays, recombinant GST-IKKε was incubated with recombinant substrate in the presence of [γ-^{32}P]ATP. Samples were then subjected to SDS-PAGE and autoradiograph analysis showing incorporation of [γ-^{32}P]ATP. Total amounts of recombinant proteins were visualized by Coomassie staining. Substrates for IKKε were full-length DDX3 or full-length IRF3 (B), full-length His-DDX3 or the indicated His-DDX3 truncation constructs (C), or recombinant His-DDX3(1–139) or His-DDX3(5–172) or the unrelated control protein His-Rab14 (D). (E) *In vitro* kinase assays were carried out as described above but in the presence of unlabeled ATP. This was followed by SDS-PAGE and WB analysis with an anti-His antibody.

none of our alanine substitution mutants displayed a complete loss of phosphorylation. We therefore also generated additional truncation mutants to narrow down the region containing the main phosphorylation site(s) for IKKε. In kinase assays with IKKε, the 80-408 and 100-408 truncation mutants retained strong phosphorylation (even though their phosphorylation was reduced by ~15% and ~37% compared to the 1-408 mutant), while constructs consisting of aa 110 onwards were not phosphorylated by IKKε (Fig. 4B). These data pinpointed the region between aa 100 and 110 as a major target site for IKKε. This region of DDX3 contains two serine residues, S102 and S109. Interestingly, S102 was predicted to be phosphorylated by both the IKKε Scansite matrix and Netphos. Our mass spectrometry results and the alanine substitution mutants also confirmed that S102 is likely an IKKε phosphorylation target. We therefore decided to mutate S102 to alanine in the context of the 80-408 truncation mutant. This 80-408 S102A mutant nearly completely lost phosphorylation by IKKε (Fig. 4C), suggesting that S102 accounts for the majority of the strong phosphorylation displayed by the 80-408 mutant.

TABLE 1 Phosphopeptides identified in IT-MSMS analysis of recombinant DDX3 or DDX3(1–408)

Phosphorylated residue(s)	Mascot score	Peptide sequence	Position of peptide
Full-length DDX3			
S70, S71, or S74	39	K.DKDAY**SS**FG**S**R.S	65–75
DDX3(1–408)			
S152 or T156	47	R.LEQELF**S**GGN**T**GINFEK.Y	146–162
S70, S71, or S74	29	K.DKDAY**SS**FG**S**R.S	65–75
S102 or S109	28	R.GR**S**DYDGIG**S**R.G	100–110
S82, S83, or S86	12	R.GK**SS**FF**S**DR.G	80–88

[a] Dots indicate trypsin cleavage sites; boldface type indicates potentially phosphorylated residues.

Serine 102 is required for the effect of DDX3 on the *ifnb* promoter. Next, we tested the interaction of our truncation and alanine mutants with IKKε and their functionality in *ifnb* reporter gene assays. Phosphorylation of the truncation mutants correlated with their ability to bind to IKKε. While DDX3(80–408) and DDX3(100–408) interacted with IKKε in His pull-down assays, the DDX3(110–408) mutant failed to bind to IKKε (Fig. 5A). We hypothesized that the interaction with IKKε would be required for DDX3 to induce *ifnb* and therefore tested our truncation mutants in *ifnb* promoter reporter gene assays. DDX3(1–408) enhanced IKKε-induced *ifnb* promoter activation similarly to full-length DDX3 (6) (Fig. 5B). As expected from the interaction data, constructs consisting of aa

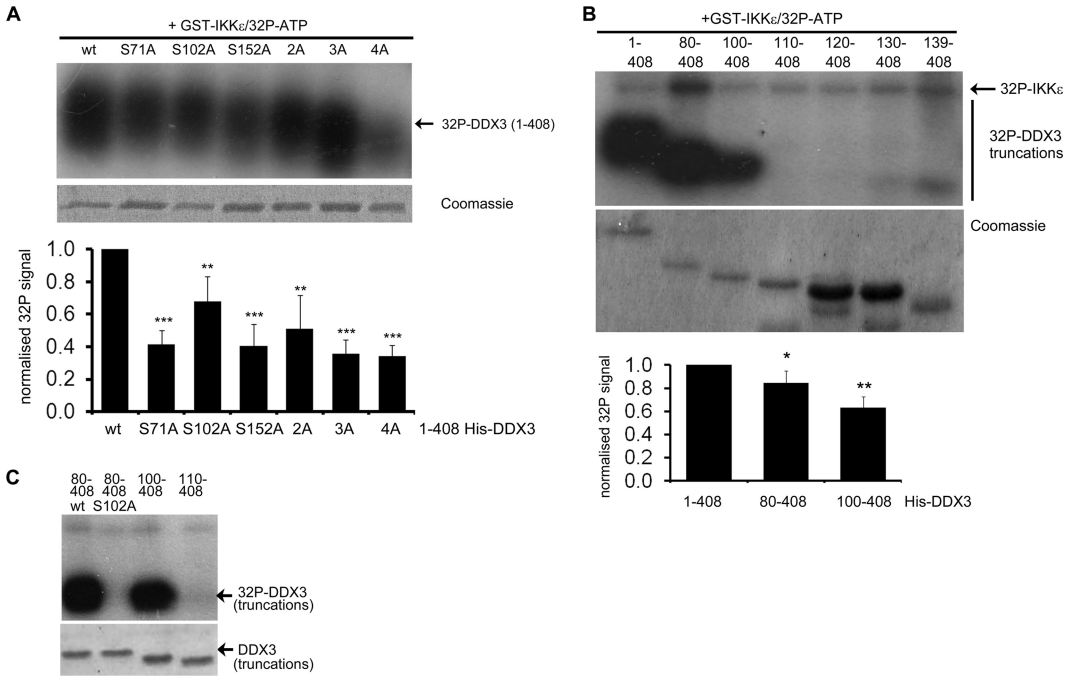

FIG 4 DDX3 is phosphorylated by IKKε on multiple sites. (A) Recombinant GST-IKKε was incubated with recombinant wild-type (wt) His-DDX3(1–408) or the indicated DDX3(1–408) alanine mutants in the presence of [γ-^{32}P]ATP. Samples were then subjected to SDS-PAGE and autoradiograph analysis. Total amounts of His-DDX3 mutants were visualized by Coomassie staining. (B) The assay was carried out as described for panel A but using the N-terminal truncation mutants of DDX3 as substrates. (A and B) The top panel shows results of one representative experiment out of four. For each repeat experiment, the intensity of autoradiograph and Coomassie-stained bands was quantified using ImageJ software. Values for autoradiograph bands were normalized to the intensity of the corresponding Coomassie-stained bands to account for differences in protein loading. The normalized signal for DDX3(1–408) was set to 1 in each case. Data in the lower panel are presented as means and standard deviations from four independent experiments. *, $P < 0.05$; **, $P < 0.01$; ***, $P < 0.001$ [all compared to wt DDX3(1–408)] by an unpaired Student's *t* test. (C) The assay was carried out as described for panel B but including the S102A mutant of DDX3(80–408).

110 onwards failed to enhance IKKε-induced *ifnb* promoter activation, while DDX3(80–408) and DDX3(100–408) still enhanced *ifnb* induction, albeit with reduced potency (Fig. 5B).

Next, we asked whether mutation of S102 in DDX3 to alanine disrupts binding to IKKε. However, all our alanine mutants, including the S102A mutant, interacted with IKKε in pulldown assays (Fig. 5C). Despite this, the three mutants containing the S102A substitution (the S102A, 3A, and 4A mutants) failed to enhance *ifnb* promoter induction (Fig. 5D). Interestingly, a phosphomimetic S102D mutant, in which serine 102 was replaced by negatively charged aspartic acid, enhanced IKKε-induced *ifnb* promoter activation similarly to wild-type DDX3 (Fig. 5D), suggesting that phosphorylation of this residue is indeed part of the mechanism. Because the S102A mutant failed to enhance *ifnb* promoter induction, we next investigated whether its interaction with IKKε is functional. To this end, we tested the S102A mutant in kinase assays, which allowed us to assess its effects on IKKε and IRF3 phosphorylation. The S102A DDX3(1–408) mutant enhanced IKKε S172 autophosphorylation similarly to wild-type DDX3 (aa 1 to 408) (Fig. 5E, top). However, despite enhanced IKKε activation, IRF3 phosphorylation was reduced in the presence of the S102A mutant compared to wild-type DDX3 (Fig. 5E, third panel). This observation made us wonder whether DDX3 has a more direct way of impacting IRF3 activation.

DDX3, but not the S102A mutant, interacts directly with IRF3. We therefore tested whether DDX3 can directly interact with IRF3. We used recombinant GST-tagged DDX3 to pull down Flag-tagged IKKε or IRF3 from cell lysates. Both IKKε and IRF3 were pulled down with DDX3 in this setup (Fig. 6A, lanes 3 and 6, respectively). We then used recombinant GST-tagged DDX3 or IKKε to confirm that their interaction with IRF3 is direct. Both IKKε and DDX3 directly interacted with recombinant His-tagged IRF3 (Fig. 6B, lanes 2 and 3, respectively). Because the S102A mutant of DDX3 retained its functional interaction with IKKε (Fig. 5C and E) but was impaired with respect to IRF3 phosphorylation and *ifnb* promoter induction (Fig. 5D and E), we next tested its interaction with IRF3. We used His-tagged recombinant IRF3 in pulldown assays with ectopically expressed wild-type DDX3 or S102A DDX3 from cell lysates. As seen before, wild-type DDX3 interacted with IRF3, while, interestingly, the S102A mutant failed to interact with IRF3 (Fig. 6C). This suggested that the defect of the DDX3 S102A mutant might lie in an inability to interact with IRF3. It also suggested that IRF3 and IKKε bind to a similar region in DDX3, and we therefore used our DDX3 truncation mutants to map its IRF3 interaction site. IRF3 failed to interact with the DDX3(100–408) and the DDX3(110–408) mutants, while IKKε bound to the DDX3(100–408) mutant but not the DDX3(110–408) mutant (Fig. 6D). This indicates that IRF3 and IKKε have adjacent and potentially overlapping, but not identical, binding sites in the N terminus of DDX3. Next, we tested whether phosphorylation of S102 is required to mediate IRF3 binding. To this end, we transfected HEK293T cells with constructs for either wild-type DDX3, the phospho-deficient S102A mutant, or the phosphomimetic S102D mu-

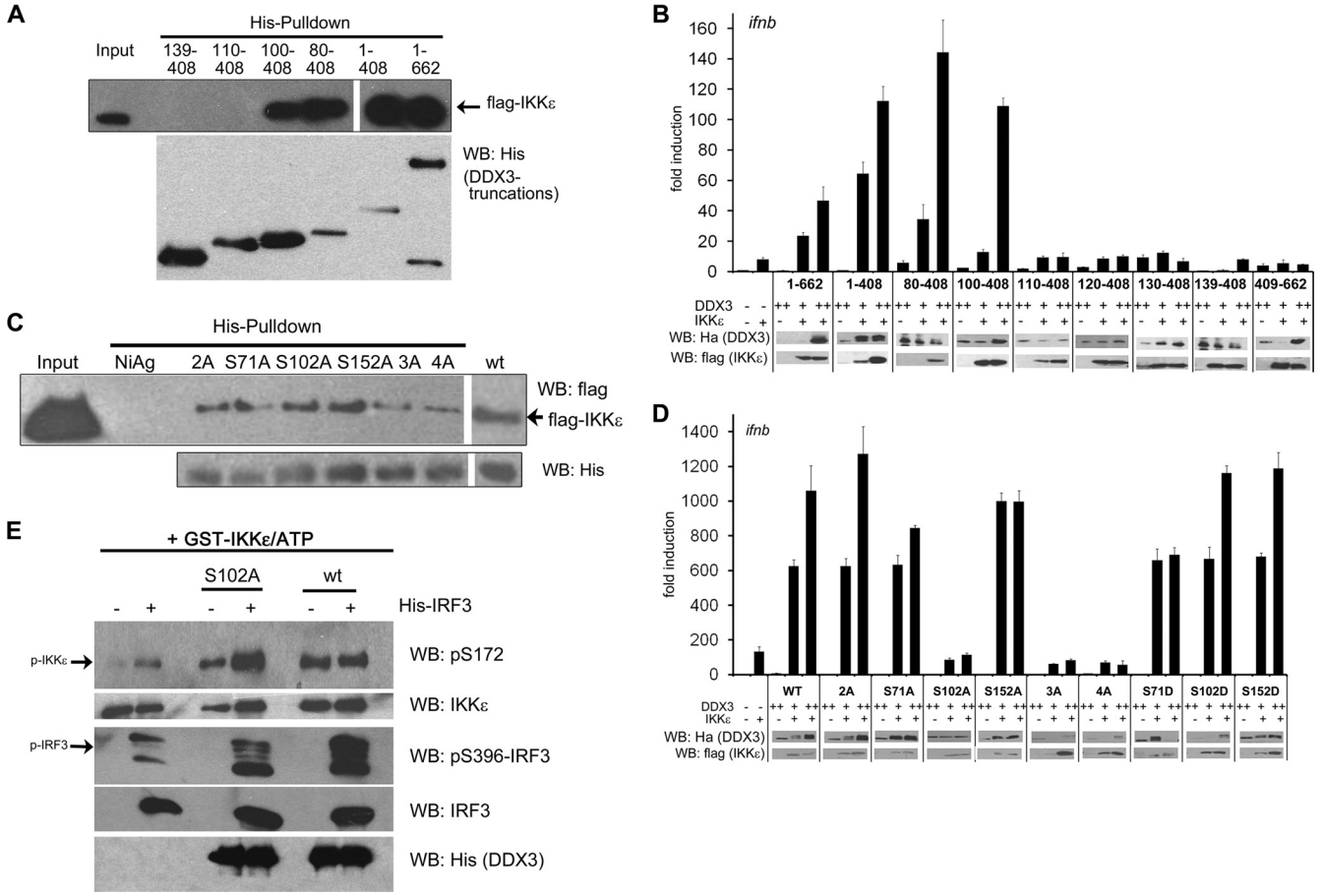

FIG 5 IKKε binding and serine 102 are required for the effect of DDX3 on the *ifnb* promoter. (A) Recombinant His-DDX3 or His-DDX3 truncation mutants were incubated with cell lysates containing Flag-IKKε. Following pulldown, interacting proteins were subjected to SDS-PAGE and Western blot (WB) analysis. The black border indicates images originate from the same autoradiography film and can be compared in intensity. (B) HEK293 cells were transfected with an *ifnb* promoter reporter gene construct and expression constructs for Flag-IKKε and HA-DDX3 or HA-DDX3 truncations. Expression of HA-DDX3 and Flag-IKKε was confirmed by WB analysis. Data for reporter gene assays are expressed as mean fold induction relative to control levels and standard deviations. Shown are results of one representative experiment out of four, performed in triplicate. (C) The assay was performed as described for panel A but using His-tagged alanine mutants of DDX3(1–408). Black borders indicate images that originated from the same autoradiography film and can be compared in intensity. (D) The assay was performed as described for panel B but testing full-length HA-tagged alanine mutants of DDX3. (E) Recombinant GST-IKKε was incubated with ATP, GST-IRF3 (aa 380 to 427), and His-DDX3(1–408) or the S102A mutant of His-DDX3(1–408). Samples were then subjected to SDS-PAGE and WB analysis. Phosphorylation of IKKε and IRF3 was detected with phospho-specific antibodies against pS172 (IKKε) and pS396 (IRF3).

tant, followed by stimulation with SeV. Cell lysates were tested for DDX3 binding to recombinant His-tagged IRF3. As seen before, the S102A mutant failed to bind to IRF3, while wild-type DDX3 and the phosphomimetic S102D mutant interacted with IRF3 (Fig. 6E). Furthermore, stimulation with SeV appeared to enhance binding of wild-type DDX3 to IRF3 and treatment with the IKKε/TBK1 inhibitor BX795 (34) prevented this effect (Fig. 6E). We concluded that S102 of DDX3 is phosphorylated by IKKε following SeV stimulation, which then facilitates the recruitment of IRF3 to the DDX3-IKKε complex. To test this hypothesis further, we transfected A549 cells with constructs for Myc-tagged DDX3 or the S102A mutant, stimulated them with SeV, and immunoprecipitated Myc-tagged DDX3/S102A. Endogenous IKKε coimmunoprecipitated with wild-type and S102A DDX3 1 h after SeV stimulation, and the interaction further increased up to 4 h after stimulation (Fig. 6F, top). Endogenous IRF3 was recruited to wild-type DDX3 but not the S102A mutant 4 h after SeV stimulation (Fig. 6F, second panel). Next, we immunoprecipitated endogenous DDX3 from A549 cells stimulated with SeV. Consistent with the semiendogenous co-IP, IKKε coimmunoprecipitated with endogenous DDX3 from 1 h after SeV stimulation (Fig. 6G, top), and the DDX3-IRF3 interaction was delayed, being detectable 8 h after SeV stimulation in this case (Fig. 6G, middle).

These interaction data support the sequential mechanism we proposed, whereby IKKε is first recruited to DDX3, followed by phosphorylation of DDX3 on S102 and subsequent recruitment of IRF3 to the phosphorylated DDX3 (Fig. 7).

Our data therefore implicate DDX3 as a scaffolding adaptor that links IKKε and IRF3 and coordinates their activation.

DISCUSSION

While we and others previously showed that the human DEAD box protein DDX3 contributes to innate immune signaling path-

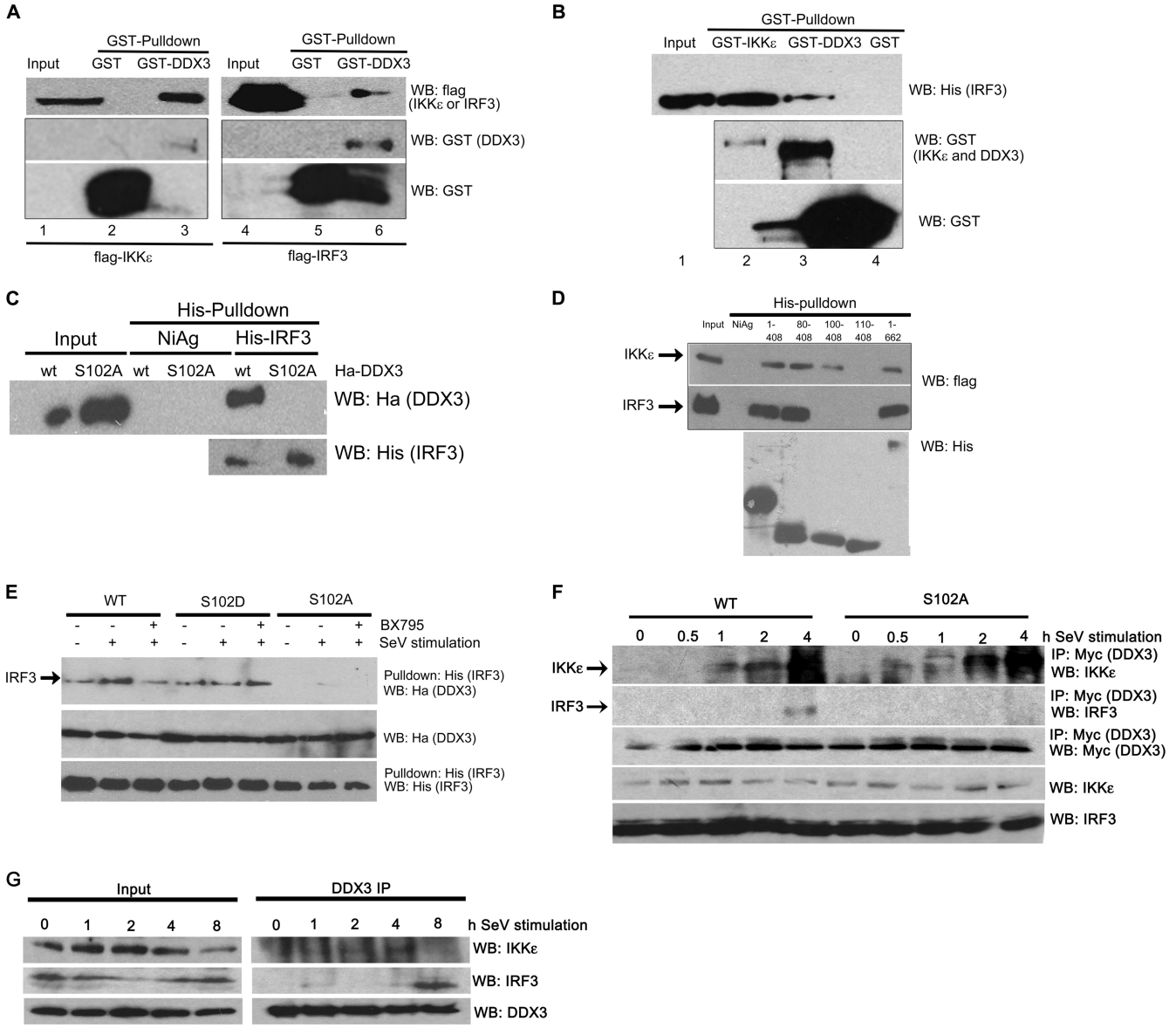

FIG 6 DDX3, but not the S102A mutant, interacts directly with IRF3. (A) Recombinant GST-DDX3 or GST was incubated with cell lysates containing Flag-IKKε or Flag-IRF3. Following pulldown, interacting proteins were subjected to SDS-PAGE and Western blot (WB) analysis. (B) Recombinant GST-DDX3, GST-IKKε, or GST was incubated with recombinant His-IRF3. Following pulldown, interacting proteins were subjected to SDS-PAGE and WB analysis. (C) Recombinant His-IRF3 was incubated with cell lysates containing HA-DDX3 or HA-DDX3 S102A. Following pulldown, interacting proteins were subjected to SDS-PAGE and WB analysis. (D) Recombinant His-DDX3 or His-DDX3 truncations were incubated with cell lysates containing Flag-IRF3 or Flag-IKKε. Following pulldown, interacting proteins were subjected to SDS-PAGE and WB analysis. (E) HEK293T cells were transfected with constructs for wild-type (WT), S102D, or S102A HA-DDX3. After 24 h, cells were stimulated with SeV for 2 h. BX795 was added 1 h before SeV stimulation (50 ng/ml). Cell lysates were used for pulldowns with recombinant His-IRF3 and complexes were subjected to SDS-PAGE and WB analysis. (F) A549 cells were transfected with constructs for either Myc-DDX3 (WT) or the Myc-DDX3 S102A mutant and stimulated with SeV as indicated. Myc-DDX3 was immunoprecipitated (IP), followed by SDS-PAGE and WB analysis. (G) A549 cells were stimulated with SeV for the indicated length of time; cell lysates were then subjected to IP with an anti-DDX3 antibody, followed by SDS-PAGE and WB analysis. (A, B, and D) Black borders indicate images originating from the same autoradiography film, which can be compared in intensity.

ways leading to IFN-β induction, its exact placement in the signaling pathways and mechanism of action was controversial. Our present study elucidated the functional relevance of the interaction between DDX3 and IKKε, and its role in IRF3 activation. We show that DDX3 binds directly to IKKε and to IRF3 and contributes to their activation. In fact, strong IRF3 phosphorylation occurred in an *in vitro* system comprising only recombinant IRF3, IKKε, and DDX3 in the presence of ATP. The N-terminal domain of DDX3(1–408) was sufficient for this and its effect on the *ifnb* promoter. While DDX3 enhanced IKKε autoactivation (as evidenced by increased phosphorylation of S172 in the activation loop of the kinase), this was only partially responsible for the increased phosphorylation of IRF3 observed in the presence of DDX3. In this context, it is important to note that activation of

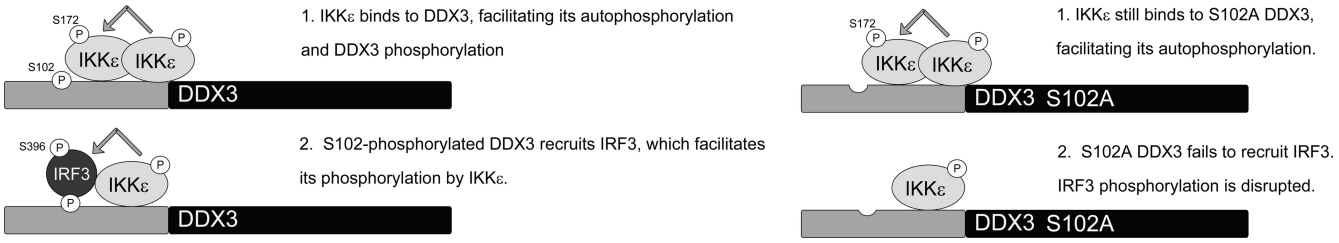

FIG 7 DDX3 acts as a scaffolding adaptor for IKKε and IRF3. Our model for the sequential mechanism by which DDX3 facilitates IKKε (1) and IRF3 (2) activation is depicted here. DDX3 first recruits IKKε, which stimulates IKKε autophosphorylation and activation. In this step, the N-terminal tail of DDX3 is phosphorylated by IKKε on multiple sites, including serine 102. The phosphorylation of S102 mediates recruitment of IRF3 to the DDX3-IKKε complex. IRF3 can subsequently be phosphorylated by IKKε and then contributes to *ifnb* promoter activation. On the right, the process is shown for the DDX3 mutant lacking S102. In this case, the physical and functional interaction with IKKε proceeds normally (1). However, due to the lack of S102 phosphorylation, IRF3 is not recruited to DDX3 and its phosphorylation is disrupted (2).

IKKε or TBK1 is not sufficient for activation of IRF3 in cells but that an additional adaptor is required for linking the activated kinases to IRF3 (17, 35). TRAF3 (TNF receptor-associated factor 3) was suggested as a candidate for this role, as it is required for IRF3 but not TBK1/IKKε activation (35). Also, in a recent study, the adaptor molecule STING, which facilitates signaling downstream of DNA receptors, was shown to link TBK1 to IRF3 (36). Interestingly, the effects of STING on TBK1 and IRF3 strongly resemble the effects we describe here for DDX3, IKKε, and IRF3. STING also mediated TBK1 and IRF3 activation in an *in vitro* reconstitution system that is essentially identical to our experimental setup (36). Interestingly, both DDX3 and STING had distinct effects on IKKε and IRF3 activation.

Effect of DDX3 on IKKε activation. With respect to its mechanism for enhancing IKKε activation, we have shown that DDX3 interacts with the scaffolding/dimerization domain (SDD) of IKKε (aa 383 to 647) and not with the C-terminal region (aa 684 to 716) that mediates binding to NAP1, TANK, and Sintbad. These adaptor proteins have also been shown to be involved in activation of TBK1 and IKKε downstream of PRRs (28). However, as they interact with a different region of IKKε, they appear to have a distinct mode of action compared to DDX3 (29, 30). It was suggested that they might recruit TBK1/IKKε to distinct subcellular locations for activation (29).

In the recently solved crystal structure of IKKβ, a kinase that is closely related to IKKε, the SDD forms an elongated α-helical region (37). The SDD mediates dimerization of the kinase and might contribute to substrate specificity. Based on their structure, the authors concluded that autophosphorylation of the activation loop could not occur within a single IKKβ dimer but was more likely to be mediated by a second IKKβ dimer in a transautophosphorylation event. Thus, higher-order arrangements of IKKβ might be required for autophosphorylation (37). It is expected that TBK1 and IKKε display a domain structure similar to that of IKKβ. Indeed, recent biochemical evidence suggests that TBK1 is activated in a similar transautophosphorylation event requiring the juxtaposition of two TBK1 dimers for phosphorylation of S172 (38). These studies suggest that a critical event for activation of the IKKs and IKK-related kinases is the positioning of kinase dimers in a conformation that allows for their transautophosphorylation.

Through its interaction with the SDD of IKKε, DDX3 could potentially stabilize such arrangements of IKKε dimers and thereby support efficient transautophosphorylation. Further biochemical studies will be required to confirm whether DDX3 indeed supports the formation of such higher-order IKKε complexes.

DDX3 also weakly interacted with the kinase domain of IKKε. This is likely because DDX3 is also a phosphorylation substrate of IKKε and therefore has to transiently interact with its kinase domain.

Phosphorylation of DDX3 by IKKε. Our data provide strong evidence that the N-terminal tail region of DDX3 is phosphorylated directly by IKKε. DDX3 has previously been identified as an interaction partner and phosphorylation target of TBK1 (7). Several TBK1 phosphorylation sites were identified within DDX3; however, most of these were located within the two RecA-like globular domains of DDX3, and none mapped to the N-terminal tail of DDX3 (7). In our hands, both the N-terminal (aa 1 to 408) and C-terminal (aa 409 to 662) domains of DDX3 interacted with IKKε, but only the N-terminal domain was strongly phosphorylated (Fig. 3C). It is likely that TBK1 and IKKε phosphorylate the same or at least overlapping residues in DDX3, and we showed that TBK1 can phosphorylate the isolated N terminus of DDX3 (aa 5 to 172) to a degree similar to that exhibited by IKKε (Fig. 3E). The published TBK1 phosphorylation sites were determined using a peptide array (7), and it is possible that specificity of phosphorylation differs in the context of larger protein domains. However, we also detected an interaction of IKKε with the C-terminal domain of DDX3 (aa 409 to 662) as well as weak phosphorylation of this domain by IKKε. It is therefore possible that the C terminus of DDX3 also contains veritable IKKε phosphorylation sites.

Here, we show that the N-terminal tail region of DDX3 that is required for *ifnb* induction undergoes strong phosphorylation by IKKε. Our N-terminal truncation mutants revealed the region between aa 100 and 110 of DDX3 as an IKKε binding site and serine 102 as a functionally important IKKε phosphorylation site. In addition, our mass spectrometry analysis and alanine substitution mutants suggested that there are multiple other phosphorylation sites for IKKε within the N terminus of DDX3, including S71, S82 or S83, and S152. It is not unusual for IKKε to phosphorylate several clustered serine residues. In IRF3, it phosphorylates at least seven serine residues within two C-terminal clusters (39). It is possible that some of these phosphorylation events are interdependent in that phosphorylated serine residues prime for subsequent phosphorylation of nearby serine residues. This interdependency could explain the significant

reductions in phosphorylation we observed with our single-alanine-substitution mutants. On the other hand, we were unable to fully abrogate phosphorylation of DDX3 by IKKε with our quadruple-alanine mutant (4A 1–408 mutant), suggesting that there might be further IKKε phosphorylation sites in the N terminus of DDX3.

In order to identify functionally important IKKε phosphorylation sites, we tested our alanine substitution mutants in *ifnb* reporter gene assays. S71 most closely matches the IKKε consensus sequence determined by Hutti et al. and was also the only phosphopeptide we identified in our mass spectrometry analysis with full-length DDX3. However, phosphorylation of the 80–408 truncation mutant was only slightly reduced compared to that of full-length DDX3, and mutation of S71 to alanine did not affect the ability of DDX3 to enhance IKKε-mediated *ifnb* promoter activation. We were initially also particularly interested in S82 and S83, as these are in the region of DDX3 that is targeted by its VACV antagonist K7. We had previously shown that mutation of the adjacent double phenylalanine motif (F84 and F85) abrogated the effect of DDX3 on the *ifnb* promoter (19). And while the S82,83A (2A) mutant displayed reduced phosphorylation by IKKε and phosphorylation of the 100–408 construct was also reduced compared to the 80–408 construct, the 2A mutant had no apparent defect with respect to *ifnb* promoter induction. It is possible that the phosphorylation of S71, S83, S82, and S152 by IKKε has subtle effects on *ifnb* induction that we failed to detect, or that there is functional redundancy between these residues. It is also possible that the phosphorylation of these residues in DDX3 affects cellular processes unrelated to *ifnb* induction. We observed increased DDX3 protein levels in the presence of IKKε (Fig. 3A); thus, it is possible that DDX3 phosphorylation by IKKε increases its stability.

In this study, we focused on serine 102 of DDX3, because the phosphodeficient S102A mutant, but not a phosphomimetic S102D mutant, failed to mediate *ifnb* promoter activation. This demonstrated that phosphorylation of S102 in DDX3 by IKKε is required for *ifnb* induction. The S102A mutant still interacted with IKKε and enhanced its autophosphorylation, but its ability to enhance IRF3 phosphorylation was reduced compared to that of wild-type DDX3 (Fig. 5E). This suggested to us that DDX3 might affect IRF3 activation more directly.

Effect of DDX3 on IRF3 activation. We show here that DDX3 directly interacts with IRF3. Interestingly, phosphorylation of DDX3 at S102 by IKKε appeared to increase the affinity of DDX3 for IRF3: the phosphodeficient S102A mutant did not interact with IRF3, while the phosphomimetic S102D mutant did (Fig. 6E). Stimulation with SeV increased the interaction between DDX3 and IRF3, which was prevented by the IKKε/TBK1 inhibitor BX795 (Fig. 6E). This provided evidence that DDX3 has to be phosphorylated by IKKε before it can bind to IRF3. Results from our coimmunoprecipitation experiments support this sequence of events: after SeV stimulation, IKKε was recruited to DDX3 first, followed by delayed IRF3 binding (Fig. 6F and G).

The failure of the S102A mutant to induce *ifnb* promoter activation suggests that the phosphorylation-induced interaction between DDX3 and IRF3 is critical for *ifnb* induction. We also demonstrate here that IKKε and IRF3 have immediately adjacent binding sites in the N-terminal region of DDX3 (Fig. 6D). We therefore propose a model whereby IKKε-mediated phosphorylation of serine 102 in DDX3 facilitates recruitment of IRF3 to DDX3. This recruitment is required for efficient IRF3 phosphorylation by IKKε, which is possibly facilitated by their juxtaposition when bound to DDX3 (Fig. 7).

DDX3 and STING act as adaptors that link activated IKK-related kinases to IRF3. As mentioned above, the protein STING has also recently been shown to facilitate IRF3 phosphorylation by TBK1. STING is required for IRF3 activation and *ifnb* induction downstream of cytosolic DNA receptors (40). There are intriguing parallels between the effects of STING on TBK1 and IRF3, as reported by Tanaka and Chen (36), and the effects of DDX3 on IKKε and IRF3 we demonstrate here. STING also enhanced both TBK1 autophosphorylation and IRF3 phosphorylation in an *in vitro* reconstitution system. Intriguingly, for both STING and DDX3, the effects on TBK1/IKKε and IRF3 activation could be uncoupled by a serine-to-alanine mutation. Mutations to Ser366 (or Leu374) in STING disrupted its effect on IRF3 activation but not on TBK1 activation (36). This is strongly reminiscent of our data for the DDX3 S102A mutant. While Tanaka and Chen found no direct evidence that S366 of STING is phosphorylated by TBK1 but suggested that STING phosphorylation by TBK1 strengthens its interaction with IRF3 (36), we demonstrate here that S102 of DDX3 is directly phosphorylated by IKKε and that this phosphorylation mediates IRF3 binding.

It thus appears that STING and DDX3 employ very similar mechanisms for coordinating activation of the IKK-related kinases and IRF3. As mentioned above, it recently emerged that an additional adaptor is required for linking the activated IKK-related kinases to IRF3 in cells (34). Both STING and DDX3 appear to be able to carry out this function. In addition to this, both of them also enhance the upstream activation of the IKK-related kinases. These two functions are distinct, because they can be uncoupled by point mutations in DDX3 (S102A) and STING. This suggests that it might be possible to target the DDX3-IRF3 interaction interface surrounding S102 therapeutically for blocking excess IFN production while leaving other IKKε- and DDX3-mediated cellular functions intact.

In summary, our study has identified a novel direct interaction between DDX3 and IRF3 that is regulated by IKKε phosphorylation of DDX3 and critical for *ifnb* induction. Our data implicate DDX3 as a bridging adaptor for IKKε and IRF3 in the RLH pathway, reminiscent of the suggested role for STING in DNA receptor pathways. It is therefore possible that STING and DDX3 belong to a group of functionally related scaffolding adaptors that coordinate activation of the IKK-related kinases and IRF3 in different signaling pathways. It will be interesting to see whether more proteins are identified that employ a similar sequential mechanism for the coordinated activation of IKKε/TBK1 and IRF3.

ACKNOWLEDGMENTS

This work was funded by a project award from the Irish Health Research Board (HRA/2009/171). A.F. is funded by a Science Foundation Ireland Research Frontiers grant (09/RFP/BIC2188). R.B. is funded through the HRB PhD Scholars Programme in Immunology (PhD/2007/9).

We thank Jessica Hutti for providing the IKKε Scansite matrix, David Fitzpatrick for advice on Scansite, John Hiscott and Qiang Sun for the GST-IRF3 (380–427) construct, Phillip Cohen for sharing unpublished reagents, and Douglas Lamont and the FingerPrints Proteomics Facility, College of Life Sciences, University of Dundee, for the mass spectrometry analysis and helpful advice.

REFERENCES

1. **Schröder M.** 2010. Human DEAD-box protein 3 has multiple functions in gene regulation and cell cycle control and is a prime target for viral manipulation. Biochem. Pharmacol. **79**:297–306.
2. **Ariumi Y, Kuroki M, Abe K, Dansako H, Ikeda M, Wakita T, Kato N.** 2007. DDX3 DEAD-box RNA helicase is required for hepatitis C virus RNA replication. J. Virol. **81**:13922–13926.
3. **Randall G, Panis M, Cooper JD, Tellinghuisen TL, Sukhodolets KE, Pfeffer S, Landthaler M, Landgraf P, Kan S, Lindenbach BD, Chien M, Weir DB, Russo JJ, Ju J, Brownstein MJ, Sheridan R, Sander C, Zavolan M, Tuschl T, Rice CM.** 2007. Cellular cofactors affecting hepatitis C virus infection and replication. Proc. Natl. Acad. Sci. U. S. A. **104**:12884–12889.
4. **Yedavalli VS, Neuveut C, Chi YH, Kleiman L, Jeang KT.** 2004. Requirement of DDX3 DEAD box RNA helicase for HIV-1 Rev-RRE export function. Cell **119**:381–392.
5. **Oshiumi H, Sakai K, Matsumoto M, Seya T.** 2010. DEAD/H BOX 3 (DDX3) helicase binds the RIG-I adaptor IPS-1 to up-regulate IFN-beta-inducing potential. Eur. J. Immunol. **40**:940–948.
6. **Schroder M, Baran M, Bowie AG.** 2008. Viral targeting of DEAD box protein 3 reveals its role in TBK1/IKK-epsilon-mediated IRF activation. EMBO J. **27**:2147–2157.
7. **Soulat D, Burckstummer T, Westermayer S, Goncalves A, Bauch A, Stefanovic A, Hantschel O, Bennett KL, Decker T, Superti-Furga G.** 2008. The DEAD-box helicase DDX3X is a critical component of the TANK-binding kinase 1-dependent innate immune response. EMBO J. **27**:2135–2146.
8. **Wang H, Ryu W-S.** 2010. Hepatitis B virus polymerase blocks pattern recognition receptor signaling via interaction with DDX3: implications for immune evasion. PLoS Pathog. **6**:e1000986. doi:10.1371/journal.ppat.1000986.
9. **Yu S, Chen J, Wu M, Chen H, Kato N, Yuan Z.** 2010. Hepatitis B virus polymerase inhibits RIG-I- and Toll-like receptor 3-mediated beta interferon induction in human hepatocytes through interference with interferon regulatory factor 3 activation and dampening of the interaction between TBK1/IKKε and DDX3. J. Gen. Virol. **91**:2080–2090.
10. **Thompson MR, Kaminski JJ, Kurt-Jones EA, Fitzgerald KA.** 2011. Pattern recognition receptors and the innate immune response to viral infection. Viruses **3**:920–940.
11. **Kawai T, Akira S.** 2007. Antiviral signaling through pattern recognition receptors. J. Biochem. **141**:137–145.
12. **O'Neill LA, Fitzgerald KA, Bowie AG.** 2003. The Toll-IL-1 receptor adaptor family grows to five members. Trends Immunol. **24**:286–290.
13. **Fitzgerald KA, McWhirter SM, Faia KL, Rowe DC, Latz E, Golenbock DT, Coyle AJ, Liao SM, Maniatis T.** 2003. IKKε and TBK1 are essential components of the IRF3 signaling pathway. Nat. Immunol. **4**:491–496.
14. **Sharma S, ten Oever BR, Grandvaux N, Zhou Lin G-PR, Hiscott J.** 2003. Triggering the interferon antiviral response through an IKK-related pathway. Science **300**:1148–1151.
15. **Johnson CL, Gale Jr, M.** 2006. CARD games between virus and host get a new player. Trends Immunol. **27**:1–4.
16. **Kato H, Sato S, Yoneyama M, Yamamoto M, Uematsu S, Matsui K, Tsujimura T, Takeda K, Fujita T, Takeuchi O, Akira S.** 2005. Cell type-specific involvement of RIG-I in antiviral response. Immunity **23**:19–28.
17. **Clark K, Peggie M, Plater L, Sorcek RJ, Young ER, Madwed JB, Hough J, McIver EG, Cohen P.** 2011. Novel cross-talk within the IKK family controls innate immunity. Biochem. J. **434**:93–104.
18. **Kalverda AP, Thompson GS, Vogel A, Schröder M, Bowie AG, Khan AR, Homans SW.** 2009. Poxvirus K7 protein adopts a Bcl-2 fold: biochemical mapping of its interactions with human DEAD box RNA helicase DDX3. J. Mol. Biol. **385**:843–853.
19. **Oda S-i, Schröder M, Khan AR.** 2009. Structural basis for targeting of human RNA helicase DDX3 by poxvirus protein K7. Structure **17**:1528–1537.
20. **Wang H, Kim S, Ryu WS.** 2009. DDX3 DEAD-box RNA helicase inhibits hepatitis B virus reverse transcription by incorporation into nucleocapsids. J. Virol. **83**:5815–5824.
21. **Mamiya N, Worman HJ.** 1999. Hepatitis C virus core protein binds to a DEAD box RNA helicase. J. Biol. Chem. **274**:15751–15756.
22. **Owsianka AM, Patel AH.** 1999. Hepatitis C virus core protein interacts with a human DEAD box protein DDX3. Virology **257**:330–340.
23. **You L-R, Chen C-M, Yeh T-S, Tsai T-Y, Mai R-T, Lin C-H, Lee Y-HW.** 1999. Hepatitis C virus core protein interacts with cellular putative RNA helicase. J. Virol. **73**:2841–2853.
24. **Oshiumi H, Ikeda M, Matsumoto M, Watanabe A, Takeuchi O, Akira S, Kato N, Shimotohno K, Seya T.** 2010. Hepatitis C virus core protein abrogates the DDX3 function that enhances IPS-1-mediated IFN-beta induction. PLoS One **5**:e14258. doi:10.1371/journal.pone.0014258.
25. **Servant MJ, Grandvaux N, ten Oever BR, Duguay D, Lin R, Hiscott J.** 2003. Identification of the minimal phosphoacceptor site required for *in vivo* activation of interferon regulatory factor 3 in response to virus and double-stranded RNA. J. Biol. Chem. **278**:9441–9447.
26. **Kishore N, Huynh QK, Mathialagan S, Hall T, Rouw S, Creely D, Lange G, Caroll J, Reitz B, Donnelly A, Boddupalli H, Combs RG, Kretzmer K, Tripp CS.** 2002. IKK-i and TBK-1 are enzymatically distinct from the homologous enzyme IKK-2. J. Biol. Chem. **277**:13840–13847.
27. **Hogbom M, Collins R, van den Berg S, Jenvert RM, Karlberg T, Kotenyova T, Flores A, Karlsson Hedestam GB, Schiavone LH.** 2007. Crystal structure of conserved domains 1 and 2 of the human DEAD-box helicase DDX3X in complex with the mononucleotide AMP. J. Mol. Biol. **372**:150–159.
28. **Ryzhakov G, Randow F.** 2007. SINTBAD, a novel component of innate antiviral immunity, shares a TBK1-binding domain with NAP1 and TANK. EMBO J. **26**:3180–3190.
29. **Goncalves A, Bürckstümmer T, Dixit E, Scheicher R, Górna MW, Karayel E, Sugar C, Stukalov A, Berg T, Kralovics R, Planyavsky M, Bennett KL, Colinge J, Superti-Furga G.** 2011. Functional dissection of the TBK1 molecular network. PLoS One **6**:e23971. doi:10.1371/journal.pone.0023971.
30. **Koop A, Lepenies I, Braum O, Davarnia P, Scherer G, Fickenscher H, Kabelitz D, Adam-Klages S.** 2011. Novel splice variants of human IKKε negatively regulate IKKε-induced IRF3 and NF-kB activation. Eur. J. Immunol. **41**:224–234.
31. **Hutti JE, Shen RR, Abbott DW, Zhou AY, Sprott KM, Asara JM, Hahn WC, Cantley LC.** 2009. Phosphorylation of the tumor suppressor CYLD by the breast cancer oncogene IKKε promotes cell transformation. Mol. Cell **34**:461–472.
32. **Obenauer JC, Cantley LC, Yaffe MB.** 2003. Scansite 2.0: proteome-wide prediction of cell signaling interactions using short sequence motifs. Nucleic Acids Res. **31**:3635–3641.
33. **Blom N, Gammeltoft S, Brunak S.** 1999. Sequence and structure-based prediction of eukaryotic protein phosphorylation sites. J. Mol. Biol. **294**:1351–1362.
34. **Clark K, Plater L, Peggie M, Cohen P.** 2009. Use of the pharmacological inhibitor BX795 to study the regulation and physiological roles of TBK1 and IκB kinase ε. J. Biol. Chem. **284**:14136–14146.
35. **Clark K, Takeuchi O, Akira S, Cohen P.** 2011. The TRAF-associated protein TANK facilitates cross-talk within the IκB kinase family during Toll-like receptor signaling. Proc. Natl. Acad. Sci. U. S. A. **108**:17093–17098.
36. **Tanaka Y, Chen ZJ.** 2012. STING specifies IRF3 phosphorylation by TBK1 in the cytosolic DNA signaling pathway. Sci. Signal. **5**:ra20.
37. **Xu G, Lo Li Y-CQ, Napolitano G, Wu X, Jiang X, Dreano M, Karin M, Wu H.** 2011. Crystal structure of inhibitor of κB kinase β. Nature **472**:325–330.
38. **Ma X, Helgason E, Phung QT, Quan CL, Iyer RS, Lee MW, Bowman KK, Starovasnik MA, Dueber EC.** 2012. Molecular basis of Tank-binding kinase 1 activation by transautophosphorylation. Proc. Natl. Acad. Sci. U. S. A. **109**:9378–9383.
39. **Chen W, Srinath H, Lam SS, Schiffer CA, Royer WE, Jr, Lin K.** 2008. Contribution of Ser386 and Ser396 to activation of interferon regulatory factor 3. J. Mol. Biol. **379**:251–260.
40. **Ishikawa H, Ma Z, Barber GN.** 2009. STING regulates intracellular DNA-mediated, type I interferon-dependent innate immunity. Nature **461**:788–792.